

3-2012

# A Simple and Inexpensive Optical Technique to Help Students Visualize Mode Shapes

Thomas R. Moore

*Department of Physics, Rollins College, TMOORE@rollins.edu*

Ashley E. Cannaday

*Rollins College*

Sarah A. Zietlow

*Paul J. Hagerty High School*

Follow this and additional works at: [http://scholarship.rollins.edu/stud\\_fac](http://scholarship.rollins.edu/stud_fac)



Part of the [Optics Commons](#), and the [Other Physics Commons](#)

---

## Published In

Thomas R. Moore, Ashley E. Cannaday and Sarah A. Zietlow, "A simple and inexpensive optical technique to help students visualize mode shapes," *Journal of the Acoustical Society of America* 131, 2480-2487 (2012).

This Article is brought to you for free and open access by Rollins Scholarship Online. It has been accepted for inclusion in Student-Faculty Collaborative Research by an authorized administrator of Rollins Scholarship Online. For more information, please contact [rwalton@rollins.edu](mailto:rwalton@rollins.edu).

# A simple and inexpensive optical technique to help students visualize mode shapes

Thomas R. Moore<sup>a)</sup> and Ashley E. Cannaday

*Department of Physics, Rollins College, 1000 Holt Avenue, Winter Park, Florida 32789*

Sarah A. Zietlow

*Paul J. Hagerty High School, 3225 Lockwood Boulevard, Oviedo, Florida 32765*

(Received 9 December 2010; revised 16 May 2011; accepted 11 August 2011)

An imaging technique is introduced that is suitable for visualizing the mode shapes of vibrating structures in an educational setting. The method produces images similar to those obtained using electronic speckle pattern interferometry (ESPI), but it can be implemented for less than 1/10 the cost of a commercial ESPI system, and the apparatus is simple enough that it can be constructed by undergraduate students. This technique allows for real-time visualization of the normal modes and deflection shapes of harmonically vibrating structures, including those with shapes that make generating Chladni patterns with sand or powder impossible. The theory of operation and construction details are discussed. © 2012 Acoustical Society of America. [DOI: 10.1121/1.3677244]

PACS number(s): 43.10.Sv, 43.40.Yq, 43.75.Yy [PSW]

Pages: 2480–2487

## I. INTRODUCTION

The importance of visualizing structural vibrations is integral to understanding acoustics, yet the most common technique for imaging vibrations in an educational setting is to place sand on a vibrating flat plate, a technique that Ernst Chladni introduced more than 200 years ago. While demonstrations with Chladni patterns are still impressive, it is surprising that with the growth in technology over the last 50 years, there is still no widely available, inexpensive method to help students visualize vibrational mode shapes. The lack of a simple and inexpensive apparatus to visualize structural vibrations hinders both education and research efforts at institutions that do not have large budgets reserved for purchasing sophisticated equipment.

Although methods do exist for visualizing structural vibrations that are superior to the method discovered by Chladni, most of these require equipment ranging in price from \$50,000 to over \$500,000. For example, scanning laser Doppler vibrometry is an effective method for visualizing steady-state structural vibrations, but the cost of such a system is several hundred thousand dollars, and building one within a reasonable time frame is beyond the capabilities of most educators. Holographic interferometry is another extremely effective method of visualizing structural vibrations; however, making holograms is tedious and time consuming, and it requires significant expertise. Additionally, the requirements for isolation from ambient vibrations, precise replacement of the hologram after development, and rigid placement of the object under study make holographic interferometry difficult to use for educational purposes. Holographic interferometry is not widely used today even for research purposes due to the inherent difficulties.

Electronic speckle pattern interferometry (ESPI) is one method of visualizing structural deflection shapes that is

widely used for research and can be used in an educational setting. This method was developed in the 1970s and has been improved upon over the past 40 years.<sup>1</sup> Like laser Doppler vibrometry and holographic interferometry, ESPI is a non-contact process that can be used to visualize the deflection shapes of vibrating structures. Unlike demonstrations with Chladni patterns, ESPI can be used to visualize the deflection shapes of objects with any orientation, and it is valuable for observing the motion of vertical surfaces and objects with non-planar surfaces. ESPI has the added advantage of allowing the real-time viewing of deflection shapes as well as the possibility of an implementation that is insensitive to small ambient vibrations.<sup>2</sup> ESPI is probably the most widely used method of visualizing the structural vibrations of objects with an area on the order of 1 m<sup>2</sup> or less, but inexpensive commercial systems can cost well in excess of \$50,000 and are therefore prohibitively expensive for most educational institutions. These and several other common methods have been recently reviewed by Molin along with some examples of their use in acoustical research.<sup>3</sup>

The purpose of this work is to describe an optical system that is easier to implement and requires less optical hardware than those methods described in Refs. 1–3 but still provides high-quality images of the mode shapes of vibrating objects in real time. It has already been shown that it is possible to build an effective electronic speckle pattern interferometer at relatively low cost (approximately \$5,000),<sup>4</sup> but recognizing that most acousticians are not experts in optical system design, the emphasis here is on simplicity. The simplicity also leads to cost reduction, making the apparatus available to institutions with limited budgets. To this end, we introduce a variation on ESPI that we have termed *two-beam speckle imaging* (TBSI).

The differences between the system described here and the ESPI systems such as those described in Ref. 3 lie in the lack of complexity and expense. A typical commercially available ESPI system requires a laser, a phase modulator, a

<sup>a)</sup>Author to whom correspondence should be addressed. Electronic mail: tmoore@rollins.edu

phase stepping device, optical fiber, hardware to insert the light into and retrieve the light from the fiber, a speckle averaging mechanism, several mirrors, and significant isolation from ambient vibrations. Most importantly, such a system also requires a specially designed lens system consisting of optical beam splitters and relay lenses that must be placed between the primary imaging lens and the recording mechanism, which is usually a CCD array. While such an optical system can be designed and built by someone skilled in optical engineering, it is unlikely that someone without graduate training in optics would be able to do so without an extensive commitment of time. Furthermore, the hardware needed to build such an apparatus is expensive.

In contrast, the system described here requires only a 50% optical beam splitter (semi-surfaced mirror), four mirrors, two lenses, and a commercially available camera lens in addition to the laser and CCD array. This method is ideal for use in educational settings because it is easy and inexpensive to implement, with a total cost less than \$3,000 (not including the cost of the computer) if all parts are purchased new. Possessing such an apparatus provides an invaluable educational tool when discussing the vibrations of structures with students.

## II. TWO-BEAM SPECKLE IMAGING

### A. Construction of a two-beam speckle imaging system

A schematic diagram of the apparatus used for TBSI is shown in Fig. 1. A beam from a laser is divided into two beams using an optical beam splitter, which is a mirror coated such that the reflectivity is 50%. One of the resulting beams is directed through a delay leg consisting of two mirrors before being expanded by a diverging lens and illuminating the object from a direction normal to the surface. The second beam is directed by two mirrors in such a manner as to illuminate the object at an angle  $\theta$  after being expanded by another diverging lens. The object that is illuminated by the two beams is imaged onto a recording device (CCD array) using a commercially available camera lens, and the image is then transferred to a computer. Once the apparatus is constructed, there are two methods of analysis that make the deflection shapes of a vibrating object visible: two beam speckle imaging (TBSI) and decorrelated two beam speckle imaging (DTBSI).

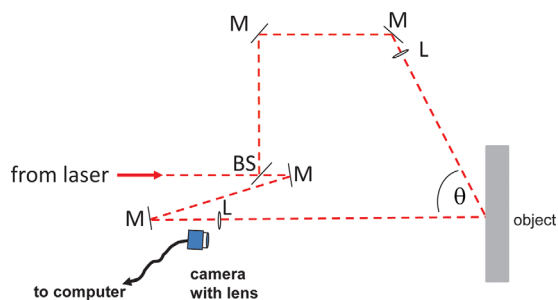


FIG. 1. (Color online) Diagram of the experimental arrangement for producing an interferogram using two beam speckle imaging. The letters in the schematic refer to lenses (L), mirror (M), and beam splitter (BS). A list of parts can be found in the appendix.

### B. TBSI

To create an interferogram that allows students to visualize the vibration of the object, an image of the object illuminated by the two beams is captured prior to the onset of vibration, and a second image is captured while the object is vibrating. Once the two images are stored in the computer, they are digitally subtracted. In the subtraction process, the value of each pixel in one image is subtracted from the value of the same pixel in the other image and the absolute value of the difference is stored as the pixel value for the resulting interferogram. For educational purposes, it is best if the image is viewed in real time, which can be accomplished by writing a computer program using any one of a variety of software packages. Indeed, it makes an excellent educational project for a student to write the software that will subtract two images and display them in real time.

Digitally subtracting the two images as described produces an image consisting of bright and dark lines, where each line represents a contour of equal vibrational amplitude. The relationship between the contour lines and the amplitude of vibration is discussed in Sec. IV. Figure 2 contains an image of a 240 mm  $\times$  240 mm  $\times$  0.6 mm flat plate mounted at the center, oscillating at a frequency of approximately 1020 Hz. For ease of imaging, the plate is mounted vertically so that the camera can be mounted on the same table. The oscillations were driven by the sound from a speaker located approximately 1 m away that was driven by a sine wave from a function generator. Because the plate was painted black, the surface has been lightly coated with a reflective layer; however, tests have shown that such a coating produces no measurable affect on the mode shapes or the resonance frequencies. For comparison purposes, a Chladni pattern of the same plate mounted horizontally on a shaker is shown in Fig. 3.

One disadvantage of this process is that the optics and the object of interest must be stable enough such that the speckle pattern does not decorrelate between the time the first image and all subsequent images are stored. This requires the optical equipment and the object of interest to

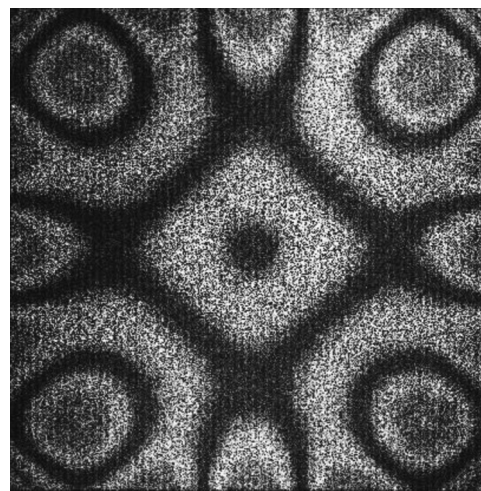


FIG. 2. TBSI interferogram of a 24cm square plate oscillating at a frequency of approximately 1020 Hz.

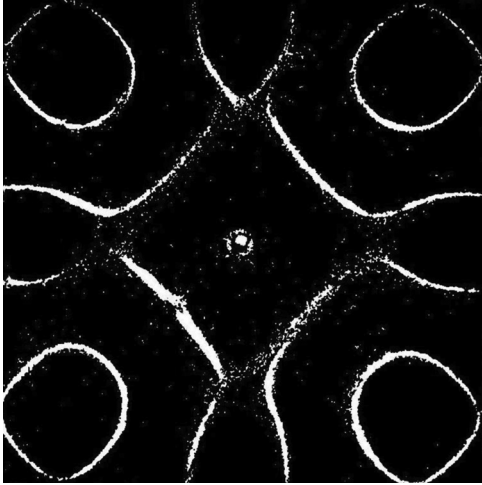


FIG. 3. Chladni pattern of the square plate shown in Fig. 2 oscillating at the same frequency. The nodal lines are made visible by sprinkling sand on the vibrating plate.

be securely mounted to the same substrate. It is sometimes helpful, although not normally necessary, for the entire apparatus to be isolated from ambient vibrations. Fortunately, there is an alternative method that eliminates the need to maintain a correlation between the images. This process, termed *decorrelated TBSI* (DTBSI), actually requires the speckle to decorrelate between capturing the two images.

### C. DTBSI

By separating the optical equipment from the object of interest, which can be accomplished by mounting them on independent tables, ambient vibration can be used to enhance the image of the deflection of the object. In fact, if there are not sufficient ambient vibrations to decorrelate the speckle pattern between images, it may be necessary to provide the necessary decorrelation. The least expensive method of decorrelating the object and the optical equipment is to mount them on separate tables and allow the ambient floor motion to decorrelate the speckle. Another option is to have a student tap one of the mirrors during the process of capturing the images. A more efficient method is to vibrate the mirror using a piezoelectric device driven at a very low frequency ( $\sim 0.2$  Hz). Alternatively, the time between image capture can be lengthened to ensure that the two images are decorrelated by random ambient motion of the object. The extent of the motion required to sufficiently decorrelate the speckle is addressed in Sec. III. The results are similar regardless of the method used to decorrelate the images.

Once the speckle has been sufficiently decorrelated between the two images, it is no longer necessary to capture and image prior to the onset of vibration. That is, when using DTBSI, both images are captured while the object is undergoing harmonic motion. If both images are captured while the object is undergoing harmonic motion, and the speckle is decorrelated between capturing the two images, the image resulting from pixel-wise subtraction produces results that are superior to those shown in Fig. 2. An image of the same plate shown in Figs. 2 and 3, captured using DTBSI, is

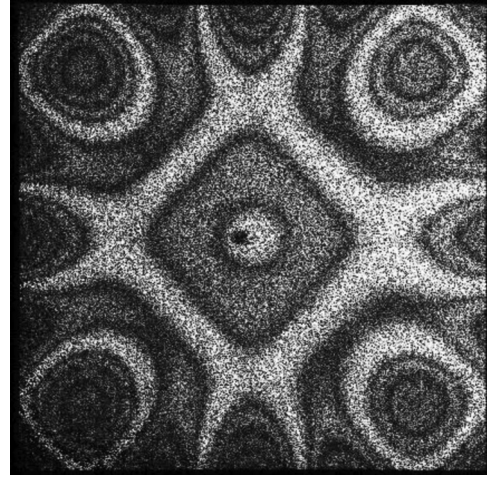


FIG. 4. DTBSI interferogram of the square plate shown in Fig. 2 oscillating at the same frequency.

shown in Fig. 4. This method is possibly the simplest, most robust, least expensive and most effective method of observing the deflection shapes of harmonically vibrating objects in an educational setting.

### D. Optical prerequisites

Because the intent is that students will actually build the apparatus described here, it is important to discuss some of the practical issues that impact the construction of the apparatus. Therefore, before discussing the theory of the interferometer we will briefly review some of the fundamental optical physics needed to understand the process.

#### 1. Speckle

Optical speckle is the granular appearance that is observed in the reflected light when coherent radiation is scattered from an optically rough surface. It is attributable to the fact that the light scattered from one part of the surface has a random phase relationship to light scattered from all the other parts of the surface. For most macroscopic objects, the characteristic surface roughness is comparable to or greater than an optical wavelength and the transverse variations usually occur on a similar length scale. This microscopic variation in surface height causes light from different parts of the object to have randomly varying path lengths from the object to the detector.

Although the presence of speckle depends upon light from different parts of the object being incident on the detector simultaneously, an object illuminated with spatially coherent radiation and imaged onto a detector will also exhibit speckle in the image even though the image plane is conjugate to the object plane. If the image was a perfect reproduction of the object, no speckle would be visible because there would be no interference effects at the image plane; however, diffraction from the limiting aperture of the imaging system causes points to be reconstructed as disks on the imaging plane. Because the surface of an object that produces a diffuse reflection is microscopically rough, the interference of the overlapping disks in the image plane creates a

speckle pattern known as subjective speckle. Because the speckle occurs due to diffraction of the limiting aperture, the average speckle size is inversely proportional to the diameter of the aperture. The relationship between the average size of the speckle  $d$  and the diameter of the aperture  $D$  is given by<sup>5</sup>

$$d = 1.22(1 + M)\frac{f\lambda}{D}, \quad (1)$$

where  $M$  is the magnification of the image,  $\lambda$  is the wavelength of the light, and  $f$  is the focal length of the imaging lens. When imaging speckle, it is necessary that the resolution of the detector be comparable to or greater than the mean speckle size.

## 2. Restrictions on optical equipment

In the following discussion, the term *coherent radiation* refers to optical radiation with a narrow enough linewidth such that illuminating the object of interest produces a static speckle pattern with high contrast. Almost all commercially available continuous-wave lasers meet this condition. The necessary laser power depends upon the size of the object and the sensitivity of the detector, but for objects with a surface area of approximately 0.1 m<sup>2</sup> (approximately 1 ft<sup>2</sup>) or less, 15 mW is usually adequate laser power when using a standard CCD camera, unless the object is dark in color. The power requirement is eased significantly if the integration time of the detector can be increased. We have found that by using an integration time of 0.067 s (1/15 s), a 15 mW laser is usually sufficient to successfully image an area of approximately 1 m<sup>2</sup> with a commercially available CCD.

Because the entire object must be illuminated, the beam produced by the laser must be expanded to cover the object of interest. This is the purpose of the lenses shown in Fig. 1. Any inexpensive positive or negative focal length lens will work well for this purpose, however, to ensure that the equipment can be contained in a small area it is helpful to use lenses with very short focal lengths. A microscope objective is useful for producing beams with a large divergence angle, but these are typically more expensive than short focal length spherical lenses.

While the lenses that expand the beams need not be of high quality, the lens used for imaging the object does need to be of relatively high quality, and it is helpful if it has an integrated aperture stop. Fortunately, inexpensive commercially available camera lenses work well. A zoom lens adds considerable flexibility but will cost two to three times as much as one with a fixed focal length. The detector is typically a CCD array, and simple board-level detectors are sufficient to achieve excellent results. ESPI images captured using an inexpensive array with an inexpensive lens have produced interferograms of sufficient quality to perform publishable research.<sup>6</sup>

Regardless of which imaging algorithm is used (TBSI or DTBSI), two-beam speckle imaging requires two beams of light to be derived from the same laser, and some of the light must be directed at an angle different from the direction normal to the surface. Therefore, mirrors and some mounting

hardware are required. The mirrors do not need to be of high quality, and the quality of the mounting hardware is not critical. Typically the mirrors and mounting hardware found in an undergraduate teaching laboratory are sufficient, and an inexpensive optical beam splitter is adequate to provide the necessary two beams. For those without access to a teaching optical laboratory, a list of the equipment used to produce the interferograms shown in Figs. 2 and 4 is included in an appendix.

In constructing the apparatus, it is important that the path difference between the two beams incident on the object not exceed the coherence length of the light, therefore a delay leg is included for the beam incident normal to the surface. The coherence length of inexpensive visible lasers can range from millimeters to meters and expensive lasers can have coherence lengths that exceed hundreds of meters, so the acceptable path difference between the two beams depends critically on which laser is used. As a rule it is best to match the path lengths of the two beams as closely as possible, but how closely they must be matched is dependent on the linewidth of the radiation. This is a parameter that is usually available from the manufacturer. Once the linewidth is known, an estimate of the coherence length can be calculated from

$$L \approx \frac{c}{\Delta\nu}, \quad (2)$$

where  $c$  is the speed of light and  $\Delta\nu$  is the linewidth. If the linewidth of the laser is unknown, it is possible to determine that the path lengths are matched sufficiently well by observing the interference between the two beams. High contrast interference indicates that the difference in path lengths is well within the coherence length of the laser. As a general rule, the path lengths should be equal to within a few millimeters, but it is not uncommon for an inexpensive HeNe laser to have a coherence length exceeding several centimeters.

In addition to being illuminated by coherent radiation, the reflection from the object of interest must be diffuse. It is often sufficient to coat the object with flat white paint, but this may not be practical for some objects, such as musical instruments, where painting can result in a significant devaluation of the object. However, some of the most significant educational uses of this technique involve observing the deflection shapes of common objects other than flat plates, so it is useful to coat the object with a white, diffusely reflective coating that can be easily removed. In cases where the object does not produce a diffuse reflection, and painting the object is not the optimal solution, a product known as Santa Snow Frost, produced by Chase Products Co. of Broadview, IL, can be used. This material is flat white and diffusely reflecting and can be easily wiped off of most objects.

## III. TBSI THEORY

The theory describing the process that results in images such as those shown in Figs. 2 and 4 is not difficult to understand, and introducing students to the theory of operation provides a rich educational opportunity. It is also useful to demonstrate the similarity between optics and acoustics as well as the importance of interdisciplinary cooperation in the sciences.

The analysis in the following text is similar to that found in Ref. (2), which describes an electronic speckle pattern interferometer. The analysis considers the response of only an infinitesimal portion of the recording device, and therefore both of the beams incident on the object can be treated as plane waves. The polarization of the two beams is assumed to be perpendicular to the optical plane of incidence (s-polarized), which means that the electric field of both beams is parallel to the surface of the object. The motion of the object is assumed to be out of the plane (in the direction of the imaging sensor), and the two beams are assumed to be coherent both temporally and spatially.

With these assumptions, and assuming that the image on the detector is conjugate to the object (i.e., the image is in focus), the irradiance at a point on the detector may be described by the superposition of the two beams incident on the object. Therefore, the usual equation for two-beam interference holds:

$$I = I_1 + I_2 + 2\sqrt{I_1 I_2} \cos(\Delta\phi), \quad (3)$$

where  $I_1$  and  $I_2$  represent the irradiance of the two beams incident on the object and  $\Delta\phi$  represents the phase difference between them.

When the object of interest is set into motion, the optical field on the detector involves a time-varying phase difference between the two beams due to the fact that the beams are incident at different angles. Assuming that the surface of the object moves with simple harmonic motion at some angular frequency  $\omega_0$ , the phase of the light that is incident normal to the surface is given by

$$\phi_1(t) = \phi_0 + \xi \sin(\omega_0 t), \quad (4)$$

and the phase of the field incident at the angle  $\theta$  to the normal is given by

$$\phi_2(t) = \xi \cos(\theta) \sin(\omega_0 t), \quad (5)$$

where the parameter  $\xi$  is the amplitude of the time-varying phase due to the motion of the surface of the object, given by

$$\xi = \frac{2\pi\Delta z}{\lambda}, \quad (6)$$

where  $\lambda$  is the wavelength of the illuminating light and  $\Delta z$  is the amplitude of the displacement. The phase angle  $\phi_0$  in Eq. 4 represents the phase difference of the two beams due to the differing path lengths of the beams to the object.

Defining  $\Delta\phi = \phi_1 - \phi_2$  and substituting Eqs. 4 and 5 into Eq. 3 yields an equation for the time-varying irradiance of a point on the detector,

$$I = I_1 + I_2 + 2\sqrt{I_1 I_2} \cos\{\phi_0 + [1 - \cos(\theta)]\xi \sin(\omega_0 t)\}. \quad (7)$$

While Eq. 7 describes the instantaneous irradiance at the detector, the interference pattern resulting from the coincidence

of the two beams is normally recorded by a device that has an integration time that is long compared to the period of the motion of the object. Therefore, the recorded image represents a time average of the interference. Provided that the irradiances of the two beams are time independent, the irradiance recorded by the detector can be described as

$$\langle I \rangle = I_1 + I_2 + 2\sqrt{I_1 I_2} \left\langle \cos\left\{ \phi_0 + [1 - \cos(\theta)]\xi \sin(\omega_0 t) \right\} \right\rangle, \quad (8)$$

where the angled brackets denote an average over the integration time of the detector. Unless the period of the motion of the object is comparable to or greater than the integration time of the detector, the irradiance recorded by the detector can be well described as a time average of the two-beam interference over the period of the motion.

The time averaged portion of Eq. 8 can be expanded to yield

$$\begin{aligned} & \left\langle \cos\left\{ \phi_0 + [1 - \cos(\theta)]\xi \sin(\omega_0 t) \right\} \right\rangle \\ &= \frac{\cos(\phi_0)}{T} \int_0^T \cos\left\{ [1 - \cos(\theta)]\xi \sin(\omega_0 t) \right\} dt \\ & \quad - \frac{\sin(\phi_0)}{T} \int_0^T \sin\left\{ [1 - \cos(\theta)]\xi \sin(\omega_0 t) \right\} dt, \quad (9) \end{aligned}$$

where  $T$  is the integration time of the detector, which is assumed to be much greater than the period of the harmonic motion; that is,

$$T \gg \frac{2\pi}{\omega_0}. \quad (10)$$

Upon integration, the second integral in Eq. 9 vanishes and integration of the remaining term reduces to

$$\langle I_1 \rangle = I_1 + I_2 + 2\sqrt{I_1 I_2} \cos(\phi_0) J_0 \left\{ [1 - \cos(\theta)]\xi \right\}, \quad (11)$$

where  $J_0$  is the zero-order Bessel function of the first kind.

To make the displacement of a harmonically vibrating object visible using TSBI, an image captured prior to the onset of motion is digitally subtracted from an image captured after motion has commenced. After subtraction, the absolute value of each pixel corresponds to the intensity displayed on the final image. When averaged over all possible values of  $\phi_0$ , this process produces an image where the value of each pixel is given by

$$I = A \left( 1 - J_0 \left\{ [1 - \cos(\theta)]\xi \right\} \right), \quad (12)$$

where  $A$  is a constant.

In the case where there is a decorrelating motion present (DTBSI), this analysis must be altered. When there is a decorrelating motion of the object, or in one of the illuminating beams, subtracting an image of the object prior to the

onset of harmonic motion from one acquired after the motion begins will not result in an image with contour lines representing out of plane motion. This is due to the fact that the speckle in the nodal regions will be different in the two images and therefore a pixel by pixel subtraction will not produce dark pixels in regions of no motion. Instead, the values of the pixels in all regions of the image will be randomly distributed in both images, and subtracting them will result in an image that is filled with random speckle.

However, if there is some decorrelating motion, the pixels in the antinodal regions will record a constant average irradiance even though the pixels in the nodal regions will not. Therefore, subtracting two images, each of which was captured while the object was executing harmonic motion, will result in the nodal regions appearing light while the antinodal regions will have lines representing contours of equal amplitude. A rigorous analysis of this case can be found in Ref. (2) for decorrelated ESPI. The analysis of DTBSI is almost identical to the analysis found in Ref. (2) with the exception of an additional  $\cos(\theta)$  term that is due to the fact that one of the beams in a DTBSI arrangement is incident off-axis. The result is that when there is decorrelating motion during the time of integration, and two images are captured while the object is undergoing harmonic motion and subsequently subtracted (pixel by pixel), the intensity of the final image is given by

$$I = A \left| J_0 \left\{ [1 - \cos(\theta)] \xi \right\} \right|. \quad (13)$$

The optimal velocity of the decorrelating motion, whether it be natural or induced, is dependent upon the wavelength of the light, the angle of the motion to the incident beams, and the integration time of the detector. Therefore, there is no single value of the velocity that will be best for every imaging situation. The interested reader should refer to Ref. (2) where a detailed analysis can be found, but because experimentation is easy and non-destructive, it is often simple to determine the optimal value with a few minutes of experimentation. Typically, motion of either the object or a mirror with a velocity of a few micrometers per second is optimal, but as is shown in Fig. 5 of Ref. (2) there will always be some visible contour lines unless

$$2T(\vec{v} \cdot \vec{k}) = N\pi, \quad (14)$$

where  $\vec{v}$  is the velocity of the decorrelating motion,  $\vec{k}$  is the wave vector of the illuminating light, and  $N$  is an integer.

In closing we note that the process of TBSI and ESPI have a close association with holographic interferometry. However, speckle pattern interferometry is fundamentally different from holographic interferometry because the physics that is responsible for the producing the interferograms is different. Holographic interferometry relies on the addition of electric fields, which interfere and are recorded as changes in the irradiance at the detector. In contrast, TBSI and ESPI both rely on subtracting images, which means that the pixel values proportional to the irradiances are subtracted. Therefore,

although ESPI is sometimes referred to as “TV holography” it is not associated with the holographic process in any way. It is also interesting to note that while speckle exists in both a holographic interferogram and a speckle pattern interferogram, it is not integral to either process and speckle averaging techniques are sometimes used to help eliminate the speckled appearance of the interferograms.

#### IV. SOME EXPERIMENTAL DETAILS

The process of building a system to produce TBSI and DTBSI images is quite simple, however, the student should be made aware that there are some physical limitations that cannot be violated. For instance, because the two beams are incident on the object at different angles, if the polarization of the light is not perpendicular to the plane of incidence (i.e., parallel to the surface of the object), the speckle contrast will be reduced by a factor of  $\cos(\theta)$ . This reduction in contrast can make it extremely difficult to observe the deflection shape of the object. Similarly, it is important that the difference in beam paths of the two beams not exceed the coherence length of the laser. If this was to happen, the speckle contrast would also be reduced. The dependence of the contrast on the path difference is complex and can even increase as the path difference exceeds the coherence length due to second order coherence effects, but the maximum contrast will always occur when the two paths are of equal length.<sup>7</sup>

There are also some improvements to the arrangement shown in Fig. 1 that result in a more flexible system, which can also be used to introduce students to some interesting physics. For example, instead of using a 50% beam splitter to create the two beams, it is possible to create a variable beam splitter by using two half-wave plates and a polarizing beam splitter. One half-wave plate can be used to adjust the relative beam intensities and the second to change the resulting p-polarized beam to s-polarization.

One of the most interesting aspect of both TBSI and DTBSI is that the amplitude of the motion corresponding to each contour line in the final image is dependent upon the angle between the two beams that are illuminating the object. This can be seen in the  $\cos(\theta)$  dependence in Eqs. 12 and 13. The result of this dependence can be seen in Fig. 4, where the number of contour lines visible in the antinodes on the right of the object are fewer than those in the similar antinode on the left. This difference is not due to some asymmetry of the vibration but to the difference in the angle that the beam subtends. The angle of the beam to the center of

TABLE I. Amplitude of vibration represented by the first five contour lines in a TBSI interferogram for three values of the angle of the incident light. The amplitude of vibration is given in terms of the number of wavelengths of the light.

Contour line from node	$\theta = 20^\circ$	$\theta = 40^\circ$	$\theta = 60^\circ$
1	10.1	2.6	1.2
2	26.8	6.9	3.2
3	43.5	11.2	5.2
4	60.1	15.5	7.2
5	76.7	19.8	9.3

TABLE II. Amplitude of vibration represented by the first five contour lines in a DTBSI interferogram for three values of the angle of the incident light. The amplitude of vibration is given in terms of the number of wavelengths of the light.

Contour line from node	$\theta = 20^\circ$	$\theta = 40^\circ$	$\theta = 60^\circ$
1	6.3	1.6	0.8
2	14.6	3.8	1.8
3	22.8	5.9	2.8
4	31.1	8.0	3.8
5	39.4	10.2	4.8

the object used to produce the interferogram shown in Fig. 4 was approximately  $60^\circ$ , but the angle of the incident beam on the right side of the object was less than it was on the left side. If the student is only interested in observing the deflection shape, this reduction in sensitivity is not important. However, if measurement of the amplitude of vibration is to be made, this dependence on angle must be considered by taking into account that  $\theta$  is a function of position on the object.

This dependence of the sensitivity of the interferometer (i.e., the out of plane displacement that corresponds to a single contour line on the interferogram) on  $\theta$  may not be important in most cases where the interferometer is being used simply as a demonstration apparatus; however, it can be exploited. When TBSI is used, each light contour line in the interferogram occurs when  $J_0\{[1 - \cos(\theta)] \xi\}$  is a minimum (nodes are black in TBSI images), and when DTBSI is used each dark contour line occurs when  $J_0\{[1 - \cos(\theta)] \xi\} = 0$  (nodes are white in DTBSI images). As the angle  $\theta$  is increased, the value of the displacement  $\Delta z$  needed to make the transition from one contour line to the next becomes smaller; therefore, it is possible to image large amplitude vibrations by reducing  $\theta$  and image smaller amplitudes by increasing  $\theta$ . The maximum sensitivity occurs when  $\theta$  approaches  $\pi/2$ , in which case the sensitivity of TBSI and DTBSI are equal to one-half the resolution of ESPI and decorrelated ESPI, respectively. The change in sensitivity with angle is shown in Tables I and II, where the amplitude of vibration that produces the first five contour lines on the interferogram is shown for three different values of  $\theta$  for TBSI and DTBSI, respectively. The amplitude is given in terms of the wavelength of the laser light.

## V. CONCLUSION

The educational value of showing students the mode shapes of common objects is significant and should not be underestimated. While Chladni patterns are impressive, it is usually more interesting to students, and sometimes more instructive, to show them the vibrational patterns of objects with which they are intimately familiar. Musical instruments are some of the most interesting and commonly available objects to use, but almost any object that can be made to produce a diffuse reflection can become an object for study when a speckle imaging system is available.

It has been shown previously that an electronic speckle pattern interferometer can be constructed with only minimal equipment.<sup>4</sup> However, a two-beam speckle imaging system such as the one presented here can produce images that are

just as impressive with even less equipment and complexity. There is also considerable educational value in having students build the apparatus as well as use it, and because the system contains so few optical components, most undergraduate laboratories will already have some of the necessary equipment. We recommend using the DTBSI technique due to its insensitivity to ambient vibrations, but there is some inherent educational value in demonstrating both techniques to students. Building the system and writing the necessary software for image subtraction is an outstanding project for an advanced undergraduate student, and it can be easily accomplished within a relatively short time span. Once built, the system can be useful for both elementary and advanced students.

## ACKNOWLEDGMENTS

This work was supported by Grant No. PHY-0964783 from the National Science Foundation.

## APPENDIX: SAMPLE PARTS LIST AND SUPPLIERS

The hardware required to construct the system shown in Fig. 1 is not extensive; however, educators with little experience in optical design and without access to an optical laboratory may find it challenging to locate the appropriate parts. Therefore, a complete list of the parts needed to construct the apparatus is shown in Table III. A good source of high-quality optical hardware is Thorlabs, Inc., in Newton, NJ. The few optical components unavailable at Thorlabs can be purchased from Edmund Optics in Barrington, NJ, or other common sources of camera equipment.

Any laser that produces light with a wavelength that can be detected by the CCD array and with power greater than 15 mW will be adequate for imaging objects with an area on the order of approximately 1 ft.<sup>2</sup> If the integration time of the detector can be increased the laser power can be significantly reduced, which can reduce the cost of the apparatus by several hundred dollars. However, for long-term versatility, we recommend a laser with more power. Laserglow Technologies (Toronto, Canada) manufactures a 200 mW diode pumped solid-state laser with a wavelength of 532 nm for less than

TABLE III. Sample hardware list for construction of TBSI apparatus.

Available from Thorlabs, Inc.	
Magnetic base	(8)
Post holder	(8)
Mounting post	(8)
Mirror with kinematic mount	(4)
Adjustable lens mount	(2)
Short focal length lens	(2)
50% beam splitter	(1)
Platform mount	(1)
Clamping arm	(1)
Mounting plate (for laser)	(1)
Available from Edmund Optics or other sources	
CCD camera (768 × 494 pixels)	(1)
c-mount lens	(1)



\$900 that works extremely well as a light source for objects with surfaces areas up to  $1 \text{ m}^2$  if the CCD has an integration time of 0.033 s, as is common.

A convenient method of mounting the necessary hardware is to use magnetic mounting bases on a steel table. These bases typically have a 1/4-20 tapped mounting hole on which post holders can be mounted; 1/2 in. diameter posts can be inserted into these post holders and the appropriate hardware attached to the top of the post with a 8-32 screw. The total cost of the hardware listed in Table III is less than \$2,000. Even if the laser must be purchased, the total cost is still under \$3,000. The expense can be reduced considerably by using a board-level camera as was demonstrated in Ref. (6). The only additional equipment required is a computer with the ability to accept input from the CCD array.

<sup>1</sup>R. Jones and C. Wykes, *Holographic and Speckle Pattern Interferometry*, 2nd ed. (Cambridge University Press, New York, 1989).

<sup>2</sup>T. Moore and J. Skubal, "Time-averaged electronic speckle pattern interferometry in the presence of ambient motion. I. Theory and experiments," *Appl. Opt.* **47**(25), 4640–4648 (2008).

<sup>3</sup>N.-E. Molin, "Optical methods for acoustics and vibration measurements," in *Handbook of Acoustics*, edited by T. Rossing (Springer, New York, 2007), pp. 1101–1123.

<sup>4</sup>T. Moore, "A simple design for an electronic speckle pattern interferometer," *Am. J. Phys.* **72**(11), 1380–1384 (2004).

<sup>5</sup>A. E. Ennos, "Speckle interferometry," in *Laser Speckle and Related Phenomena*, edited by J. C. Dainty (Springer, New York, 1984), pp. 203–253.

<sup>6</sup>N. Timme and A. Morrison, "The mode shapes of a tennis racket and the effects of vibration dampers on those mode shapes," *J. Acoust. Soc. Am.* **125**(6), 3650–3656 (2009).

<sup>7</sup>E. Hect, in *Optics*, fourth ed. (Addison Wesley, San Francisco, 2002), pp. 560–578.